




## Article

# Argentopolybasite, $\text{Ag}_{16}\text{Sb}_2\text{S}_{11}$ , a new member of the polybasite group

Martin Števko<sup>1,2\*</sup> , Tomáš Mikuš<sup>3</sup>, Jiří Sejkora<sup>2</sup> , Jakub Plášil<sup>4</sup> , Emil Makovický<sup>5</sup>, Jozef Vlasáč<sup>3</sup>   
and Anatoly Kasatkin<sup>6</sup>

<sup>1</sup>Earth Science Institute v.v.i., Slovak Academy of Sciences, Dúbravská cesta 9, P. O. BOX 106, 840 05 Bratislava, Slovakia; <sup>2</sup>Department of Mineralogy and Petrology, National Museum, Cirkusová 1740, 193 00 Prague 9 – Horní Počernice, Czech Republic; <sup>3</sup>Earth Science Institute v.v.i., Slovak Academy of Sciences, Ďumbierska 1, 974 11 Banská Bystrica, Slovakia; <sup>4</sup>Institute of Physics of the CAS, v.v.i., Na Slovance 1999/2, 182 21 Prague 8, Czech Republic; <sup>5</sup>Department of Geosciences and Resource Management, University of Copenhagen, Østervoldgade 10, DK-1350, Copenhagen, Denmark; and <sup>6</sup>Fersman Mineralogical Museum of the Russian Academy of Sciences, Leninsky Prospekt 18-2, 119071 Moscow, Russia

### Abstract

The new mineral argentopolybasite, ideally  $\text{Ag}_{16}\text{Sb}_2\text{S}_{11}$ , was found at the Kremnica Au–Ag epithermal deposit, Žiar nad Hronom Co., Banská Bystrica Region, Slovakia (type locality), Šibeničný vrch near Nová Baňa, Žarnovica Co., Banská Bystrica Region, Slovakia (cotype locality) and the Arykevaam epithermal Au–Ag deposit, Anadyr' District, Chukotka Autonomous Okrug, Russian Federation (cotype locality). At the Kremnica deposit argentopolybasite was found as discrete, well-developed (pseudo)hexagonal tabular crystals up to 4 mm in size or as complex crystalline aggregates and groups up to 5 mm in size in cavities of quartz. It is associated with pyrargyrite, polybasite, stephanite, miargyrite, rozhdstvenskayaite-(Zn), argentotetrahedrite-(Zn), naumannite, gold and pyrite. Argentopolybasite is dark grey to black, with a black streak and metallic to opaque lustre. The Mohs hardness is ~3. It is brittle with no observable cleavage and with a conchoidal fracture. The calculated density is  $6.403 \text{ g}\cdot\text{cm}^{-3}$ . In reflected light, argentopolybasite is grey, with no observable bireflectance and very weak pleochroism. It shows moderate anisotropy in crossed polarisers with weak greenish and green–blue tints. The reflectance values for wavelengths recommended by the Commission on Ore Mineralogy of the IMA are ( $R_{\min}/R_{\max}$ , %): 30.3/31.0 (470 nm), 28.8/29.3 (546 nm), 28.1/28.6 (589 nm) and 27.4/27.8 (650 nm). The empirical formulae (based on 29 apfu) are, Kremnica:  $(\text{Ag}_{15.94}\text{Cu}_{0.18})_{\Sigma 16.12}(\text{Sb}_{1.40}\text{As}_{0.61})_{\Sigma 2.01}(\text{S}_{10.60}\text{Se}_{0.25}\text{Cl}_{0.03})_{\Sigma 10.88}$ , Nová Baňa:  $\text{Ag}_{16.30}(\text{Sb}_{1.74}\text{As}_{0.22})_{\Sigma 1.96}(\text{S}_{10.69}\text{Cl}_{0.04})_{\Sigma 10.73}$  and Arykevaam:  $(\text{Ag}_{15.54}\text{Cu}_{0.38})_{\Sigma 15.92}(\text{Sb}_{1.56}\text{As}_{0.51})_{\Sigma 2.07}\text{S}_{11.01}$ . The ideal end-member formula for argentopolybasite is  $\text{Ag}_{16}\text{Sb}_2\text{S}_{11}$ . Argentopolybasite is trigonal, space group  $P321$ ,  $a = 15.0646(5) \text{ \AA}$ ,  $c = 12.2552(5) \text{ \AA}$ ,  $V = 2408.61(15) \text{ \AA}^3$  and  $Z = 2$ . The seven strongest powder X-ray diffraction lines are [ $d_{\text{obs}}$  in  $\text{ \AA}$ , (I),  $hkl$ ]: 12.169, (40), 001; 3.162, (100), 041; 3.045, (54), 004; 2.881, (45), 042; and 2.4256, (28), 421. The crystal structure of argentopolybasite from Kremnica, refined to  $R_{\text{obs}} = 0.0741$  for 2804 observed reflections, confirmed that the atomic arrangement is isotypic to that of the other members of the polybasite group and it is isostructural with argentepearceite.

**Keywords:** argentopolybasite, new mineral, polybasite group, sulfosalts, crystal structure, epithermal mineralisation, Kremnica, Slovakia

(Received 13 April 2022; accepted 12 December 2022; Accepted Manuscript published online: 17 February 2023;  
Associate Editor: Ian Terence Graham)

### Introduction

Argentopolybasite, ideally  $\text{Ag}_{16}\text{Sb}_2\text{S}_{11}$ , is a new member of the polybasite group. The type locality of argentopolybasite is the Kremnica Au–Ag epithermal deposit in Slovakia. It was also identified at two other (cotype) localities in Slovakia and the Russian Federation.

Argentopolybasite is named in accordance with the existing nomenclature scheme for the polybasite-group minerals (Bindi *et al.*, 2007c). As this new mineral has  $\text{Sb} > \text{As}$  and the structural position 'Cu' of the B module layer is dominated by Ag, it has

been named argentopolybasite to indicate that it is the Ag-dominant analogue of polybasite and, at the same time, the Sb-dominant analogue of the recently defined argentepearceite (Sejkora *et al.*, 2020). Moreover, as it exhibits the 221 unit-cell type, the full name for the polytype is argentopolybasite- $T2ac$ , the Ag-dominant analogue of polybasite- $T2ac$  (Bindi *et al.*, 2007c). The new mineral and its name (symbol  $\text{Aplb-}T2ac$ ) have been approved by the Commission on New Minerals, Nomenclature and Classification of the International Mineralogical Association (IMA2021-119, Števko *et al.*, 2022). The holotype specimen (polished section) of argentopolybasite is deposited in the collections of the Department of Mineralogy and Petrology, National Museum in Prague, Cirkusová 1740, 19300 Praha 9, Czech Republic under the catalogue number P1P 59/2021; cotype sample from Nová Baňa in the same collection (the catalogue number P1P 60/2021); cotype sample from Arykevaam in the collection of Fersman

\*Author for correspondence: Martin Števko, Email: [mminerals@gmail.com](mailto:mminerals@gmail.com)

Cite this article: Števko M., Mikuš T., Sejkora J., Plášil J., Makovický E., Vlasáč J. and Kasatkin A. (2023) Argentopolybasite,  $\text{Ag}_{16}\text{Sb}_2\text{S}_{11}$ , a new member of the polybasite group. *Mineralogical Magazine* 87, 382–395. <https://doi.org/10.1180/mgm.2022.141>

© The Author(s), 2023. Published by Cambridge University Press on behalf of The Mineralogical Society of the United Kingdom and Ireland. This is an Open Access article, distributed under the terms of the Creative Commons Attribution licence (<http://creativecommons.org/licenses/by/4.0/>), which permits unrestricted re-use, distribution and reproduction, provided the original article is properly cited.

Mineralogical Museum of the Russian Academy of Sciences, Moscow, Russia (registration number 5818/1).

## Occurrence

Argentopolybasite was found at three different localities: Kremnica Au–Ag epithermal deposit, Žiar nad Hronom Co., Banská Bystrica Region, Slovakia (48°43'1"N, 18°53'52"E – type locality), Šibeničný vrch near Nová Baňa, Žarnovica Co., Banská Bystrica Region, Slovakia (48°24'49"N, 18°38'14"E – cotype locality), and the Arykevaam epithermal Au–Ag deposit, Anadyr' District, Chukotka Autonomous Okrug, Russian Federation (66°43'00.8"N, 172°02'13.2"E – cotype locality).

The Kremnica epithermal Au–Ag deposit is located in the vicinity of Kremnica town, in the northern part of the Central Slovakian Volcanic Field, which comprises the remnants of a large Miocene andesite stratovolcano (Lexa *et al.*, 1998). The Kremnica deposit consists of a system of low-sulfidation epithermal veins with Au–Ag–Sb mineralisation developed on marginal faults in the eastern part of the Kremnica resurgent horst. Two principal vein systems were distinguished: (1) 1<sup>st</sup> vein system, which is located NW of Kremnica town, and is dominated by a first-order listric fault, intruded by rhyolite dykes, and (b) 2<sup>nd</sup> vein system, which extends underneath the town of Kremnica and is represented by a large-scale complementary vein system with 40 veins in the hanging wall of the listric fault (Böhmer, 1966; Kraus *et al.*, 1999; Lexa and Bartalský, 1999; Koděra *et al.*, 2007). The samples with argentopolybasite were collected by Martin Števko in 2008 from a thin (up to 10 cm wide) hydrothermal quartz vein, located in the Václav-north adit, in the central part of the 1<sup>st</sup> vein system. This vein frequently contained drusy cavities with crystalline quartz, dolomite, siderite and abundant aggregates and crystals of Ag sulfosalts (argentopolybasite, polybasite, pyrargyrite, argentotetrahedrite-(Zn), rozhdestvenskayaite-(Zn) and a potentially new species 'rozhdestvenskayaite-(Fe)' as well as minor stephanite and miargyrite) and subordinate amounts of gold, naumannite and pyrite.

Epithermal veins with Ag–Au mineralisation at the Nová Baňa are located in the western part of the Middle Miocene Štiavnica stratovolcano, represented mainly by andesitic rocks. The deposit is developed on the N–S oriented fault system that gradually divides a local horst in the west from a subsident part in the east. Low- to intermediate-sulfidation epithermal veins and veinlets are hosted in the extrusive rhyolite body of the Jastrabá Formation (Messinian) in the central part of the deposit. In the SE (Gupňa) and SW (Šibeničný vrch) parts of the deposit, the host rocks comprise ignimbrites and andesites (Tortonian) of the first stage of the stratovolcano evolution (Konečný *et al.*, 1998; Lexa *et al.*, 2002; Chernyshev *et al.*, 2013). The ore-bearing structures in Nová Baňa have mostly NNE–SSW strike and dip steeply to the east. The largest vein structures follow the contact of the rhyolite intrusion and older andesites, attaining a length of ~1 km and thickness up to 50 m (Majzlan *et al.*, 2018). The samples containing argentopolybasite were collected from the dumps of old workings on the Johana and Krakauer vein at the eastern slope of the Šibeničný vrch. The ore shows a typical signature of low-sulfidation epithermal mineralisation with banded textures composed of 'adularia', chalcedony-like quartz and disseminated precious metal minerals. Argentopolybasite is associated with acanthite, pyrargyrite, proustite, rozhdestvenskayaite-(Zn), naumannite and Au–Ag alloys.

The Arykevaam epithermal Au–Ag deposit is located in the Arctic zone of the Russian Far East, 340 km northeast of the district centre, Anadyr' town and occupies an approximate area of 2 × 2 km. Geologically, it is located on the eastern flank of a dome-shaped volcanic structure composed of various Upper Cretaceous volcanics ranging from basalts to subalkaline rhyolites. Subvolcanic and vent formations of predominantly acidic composition are confined to areas of arcuate and linear tectonic faults striking at different azimuths. The outcrops of subvolcanic bodies are associated spatially with fields of secondary quartzites and mudstones that contain quartz veins with epithermal gold–silver mineralisation. The main vein mineral is quartz. 'Adularia', chlorite, 'hydromica', kaolinite and gypsum are present in minor amounts. The main ore minerals are pearceite and polybasite, whereas acanthite, minerals of the freibergite series, proustite, chalcopyrite, galena, pyrite, sphalerite and native gold are less common (Volkov *et al.*, 2020). The sample containing argentopolybasite was collected in the summer 2020 by Evgeniy A. Vlasov.

Argentopolybasite is a hydrothermal mineral, which formed from low- (Kremnica, Nová Baňa) to moderate-temperature (Arykevaam) hydrothermal solutions.

## Physical and optical properties

At the Kremnica deposit argentopolybasite was found as discrete, well-developed (pseudo)hexagonal tabular crystals up to 4 mm in size or as complex crystalline aggregates and groups up to 5 mm in size (Fig. 1). At the Nová Baňa deposit, argentopolybasite occurs as anhedral grains up to 0.3 mm in size with thin rims of acanthite (Fig. 2) and at the Arykevaam deposit it forms tabular crystals up to 1.5 mm (Fig. 3) or zones up to 0.3 × 0.2 mm developed in Ag-rich and Cu-poor polybasite grains up to 1 cm across enclosed in a quartz matrix. Argentopolybasite is dark grey to black, opaque, with a black streak, a metallic to opaque lustre and it is non-fluorescent in shortwave and longwave ultraviolet light. The Mohs hardness is estimated at ~3 based on scratch tests and by analogy to other polybasite-group minerals. Crystals of argentopolybasite show no cleavage and are very brittle with a typical conchoidal fracture. A density of 6.403 g·cm<sup>-3</sup> was calculated using the ideal empirical formula and unit-cell volume refined from the single-crystal X-ray diffraction data. Argentopolybasite is grey in reflected light with no visible



**Figure 1.** Group of well-developed, pseudo-hexagonal tabular crystals of argentopolybasite from Kremnica. Associated minerals are quartz, dolomite and minor pyrargyrite. Field of view is 5 mm. Photo: P. Skácha.

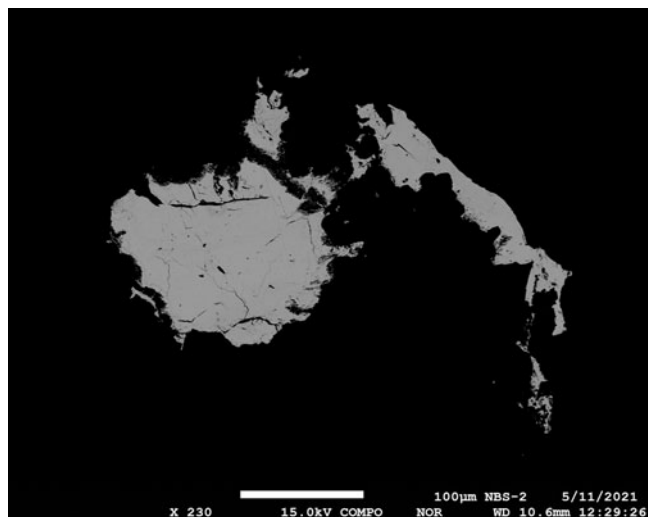


**Figure 2.** Anhedral grains of argentopolybasite from Nová Baňa. Back-scattered electron photo: T. Mikuš.

bireflectance and very weak pleochroism. It shows moderate anisotropy in crossed polarisers with weak greenish and green-blue tints and no internal reflections. Reflectance values measured in the air using a spectrophotometer MSP400 Tidas on a Leica microscope, with a 50× objective, are given in Table 1 and shown in Fig. 4 and in Fig. 5 compared with published data for polybasite.

### Chemical composition

Quantitative chemical analyses were carried-out using a Cameca SX100 electron microprobe (wavelength dispersive spectroscopy (WDS) mode, 25 kV, 4 nA and 15 µm beam diameter) at the National Museum Prague, Czech Republic (samples from Kremnica and Nová Baňa) and Cameca SX100 electron microprobe (WDS mode, 25 kV, 10 nA and 2 µm beam diameter) at the Department of Geological Sciences, Faculty of Science, Masaryk University, Brno, Czech Republic (Arykevaam sample). Results for the samples from Kremnica (average of 12 spot analyses), Nová Baňa (average of 10 spot analyses) and Arykevaam (8 spot analyses) are given in Table 2. Contents of other elements



**Figure 3.** Tabular crystal of argentopolybasite on quartz from Arykevaam deposit. Field of view is 2.5 mm. Photo: M. Milshina.

**Table 1.** Reflectance data for argentopolybasite from Kremnica.\*

$R_{\max}$	$R_{\min}$	$\lambda$ (nm)	$R_{\max}$	$R_{\min}$	$\lambda$ (nm)
32.2	31.7	400	29.0	28.6	560
32.2	31.6	420	28.7	28.3	580
31.8	31.3	440	<b>28.6</b>	<b>28.1</b>	<b>589</b>
31.3	30.6	460	28.4	28.0	600
<b>31.0</b>	<b>30.3</b>	<b>470</b>	28.2	27.7	620
30.7	30.1	480	27.9	27.5	640
30.2	29.7	500	<b>27.8</b>	<b>27.4</b>	<b>650</b>
29.8	29.3	520	27.6	27.2	660
29.3	28.9	540	27.2	26.9	680
<b>29.3</b>	<b>28.8</b>	<b>546</b>	26.9	26.5	700

\*The reference wavelengths required by the Commission on Ore Mineralogy (COM) are given in bold

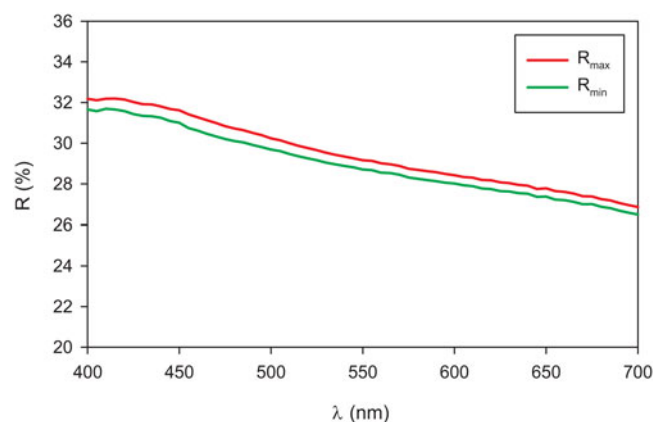


**Figure 4.** Reflectivity curves for argentopolybasite from Kremnica.

with atomic numbers higher than that of carbon are below detection limits. Matrix correction by PAP software (Pouchou and Pichoir, 1985) was applied to the data. The calculated empirical formulae of argentopolybasite based on 29 atoms per formula unit (apfu) are: Kremnica:  $(\text{Ag}_{15.94}\text{Cu}_{0.18})_{\Sigma 16.12}(\text{Sb}_{1.40}\text{As}_{0.61})_{\Sigma 2.01}(\text{S}_{10.60}\text{Se}_{0.25}\text{Cl}_{0.03})_{\Sigma 10.88}$ ; Nová Baňa:  $\text{Ag}_{16.30}(\text{Sb}_{1.74}\text{As}_{0.22})_{\Sigma 1.96}(\text{S}_{10.69}\text{Cl}_{0.04})_{\Sigma 10.73}$ ; and Arykevaam:  $(\text{Ag}_{15.54}\text{Cu}_{0.38})_{\Sigma 15.92}(\text{Sb}_{1.56}\text{As}_{0.51})_{\Sigma 2.07}\text{S}_{11.01}$ . The ideal end-member formula for argentopolybasite is  $\text{Ag}_{16}\text{Sb}_2\text{S}_{11}$ , which requires Ag 74.33, Sb 10.49 and S 15.19, total 100.00 wt.%.

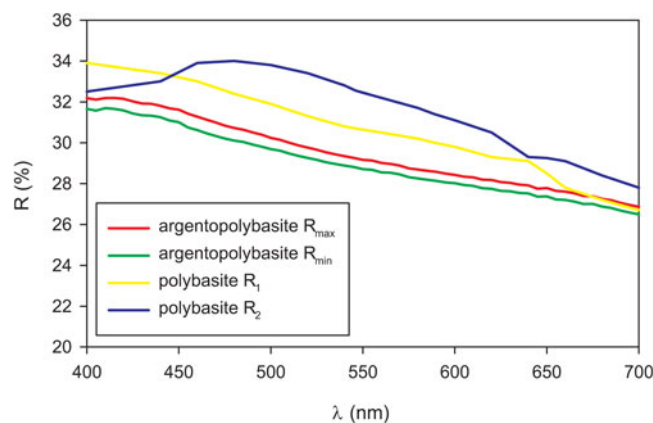


**Figure 5.** Reflectivity curves for argentopolybasite from Kremnica compared with published data for polybasite (Criddle and Stanley, 1993) from Guanajuato, Mexico (chemical composition is not given).

**Table 2.** Chemical composition (in wt.%) of argentopolybasite from Kremnica, Nová Baňa and Arykevaam.

Constituent	Mean	Range	S.D. ( $\sigma$ )	Reference material
Kremnica (holotype)				
Ag	74.22	73.37–75.35	0.67	Ag
Cu	0.49	0.14–0.89	0.20	CuFeS <sub>2</sub>
As	1.97	1.64–2.33	0.24	NiAs
Sb	7.33	6.64–7.93	0.36	Sb <sub>2</sub> S <sub>3</sub>
S	14.67	14.20–14.94	0.20	CuFeS <sub>2</sub>
Se	0.85	0.50–1.12	0.20	PbSe
Cl	0.05	0–0.13	0.05	NaCl
Total	99.58			
Nová Baňa (cotype)				
Ag	75.10	74.08–76.01	0.74	Ag
Cu	0.00			CuFeS <sub>2</sub>
As	0.71	0.10–1.49	0.40	NiAs
Sb	9.06	8.02–9.62	0.59	Sb <sub>2</sub> S <sub>3</sub>
S	14.64	14.11–15.12	0.29	CuFeS <sub>2</sub>
Cl	0.07	0–0.11	0.03	NaCl
Total	99.58			
Arykevaam (cotype)				
Ag	73.55	73.05–73.99	0.37	Ag
Cu	1.07	0.92–1.20	0.10	CuFeS <sub>2</sub>
As	1.68	0.90–2.25	0.55	pararammelsbergite
Sb	8.32	7.19–9.23	0.74	Sb
S	15.48	15.37–15.62	0.11	FeS <sub>2</sub>
Total	100.10			

S.D. – standard deviation

### X-ray crystallography and structure refinement

Powder X-ray diffraction data for argentopolybasite from Kremnica were recorded at room temperature using a Bruker D8 Advance diffractometer equipped with a solid-state LynxEye detector and secondary monochromator producing CuK $\alpha$  radiation housed at the Department of Mineralogy and Petrology, National Museum, Prague, Czech Republic. The instrument was operating at 40 kV and 40 mA. In order to minimise the background, the powder sample was placed on the surface of a flat silicon wafer. The powder pattern of argentopolybasite was collected in the Bragg–Brentano geometry in the range 3–75°2 $\theta$  CuK $\alpha$ , step 0.01° and counting time of 20 s per step (total duration of the experiment was ca. 30 hours). The positions and intensities of diffractions were found and refined using the Pearson VII profile-shape function of the ZDS program package (Ondruš, 1993) and the unit-cell parameters were refined by the least-squares program of Burnham (1962). The powder X-ray diffraction data of argentopolybasite from Kremnica presented in Table 3 show good agreement with the pattern calculated from the structure determination. Unit-cell parameters of argentopolybasite from Kremnica refined for the trigonal space group *P*321 (#150) are:  $a = 15.112(2)$  Å,  $c = 12.174(5)$  Å,  $V = 2407.7(9)$  Å<sup>3</sup> and  $Z = 4$ .

Single-crystal X-ray studies of argentopolybasite were carried-out using a Rigaku SuperNova single-crystal diffractometer with Atlas S2 CCD detector and monochromatised MoK $\alpha$  radiation from the microfocus X-ray tube. A plate-like single-crystal fragment of argentopolybasite from Kremnica with approximate dimensions 58 × 24 × 23  $\mu$ m, was separated from a polished section of an aggregate pre-analysed by means of electron microprobe and was mounted on a glass fibre. Data reduction was performed using *CrysAlisPro* Version 1.171.39.46 (Rigaku, 2019). The data were corrected for Lorentz factor, polarisation effect and absorption (multi-scan, *ABSPACK* scaling algorithm; Rigaku, 2019).

**Table 3.** Powder X-ray diffraction data ( $d$  in Å) for argentopolybasite from Kremnica.\*

$l_{\text{meas}}$	$d_{\text{meas}}$	$d_{\text{calc}}$	$hkl$
<b>40</b>	<b>12.169</b>	12.174	001
5	6.553	6.544	200
15	6.085	6.087	002
12	4.581	4.583	211
3	3.632	3.630	310
17	3.276	3.272	400
9	3.208	3.210	222
<b>100</b>	<b>3.162</b>	3.160, 3.160	041, 401
<b>54</b>	<b>3.045</b>	3.043	004
18	2.918	2.915, 2.915	231, 321
<b>45</b>	<b>2.881</b>	2.882, 2.882	042, 402
23	2.691	2.693, 2.693	322, 232
22	2.547	2.547, 2.547	403, 043
<b>28</b>	<b>2.4256</b>	2.4238	421
7	2.3704	2.3701	224
7	2.2274	2.2284, 2.2284	404, 044
6	2.1143	2.1120	243
7	2.0489	2.0466	225
22	1.8864	1.8890	440
6	1.8690	1.8667	441
4	1.7391	1.7393, 1.7393	622, 262
6	1.7117	1.7126	443
2	1.6217	1.6214	081
2	1.6031	1.6050	444
12	1.5172	1.5173, 1.5173	083, 803
8	1.4925	1.4925	445

\*The strongest lines are given in bold

The structure of argentopolybasite was solved from the diffraction data using the intrinsic phasing by *SHELXT* program (Sheldrick, 2015) and refined using the software *Jana2020* (Petříček *et al.*, 2020). The refined unit-cell metrics indicated that the studied crystal belongs to the trigonal polytype *-T2ac* (Bindi *et al.*, 2007a, 2007c) and that it should actually be an Sb-dominant analogue of argentopearceite (Sejkora *et al.*, 2020). Nevertheless, in the case of the crystal studied, we found that the situation is actually more complex than for argentopearceite, in which the twinning was not so complicated (only by lowered syngony due to the absence of the inversion centre). The argentopolybasite crystal currently studied was found to be twinned by metric merohedry (diffraction type I; Petříček *et al.*, 2016) as a four-fold twin (Fig. 6; Table 4); all symmetry elements connected with the higher hexagonal symmetry were found to be non-vanished. Along with the use of the higher-order anharmonic Gram–Charlier tensors for the description of Debye–Waller factors of Ag atoms (this approach has been described elsewhere, see e.g. Evain *et al.*, 2006; Bindi *et al.*, 2013, 2015a, 2015b), the refinement of the structure model converged to very acceptable values:  $R_{\text{obs}} = 0.0741$ ,  $wR_{\text{obs}} = 0.1746$ ,  $R_{\text{all}} = 0.1029$  and  $wR_{\text{all}} = 0.1873$  for 2804 [ $I > 3\sigma(I)$ ] and 4339 reflections and 304 refined parameters, respectively; the remaining residuals in the difference-Fourier maps are 3.49 and  $-1.07 e^{-}\cdot\text{Å}^{-3}$ . We report the experimental details and crystal data in Table 4, and atomic positions in Table 5. Anisotropic and high-order displacement parameters (up to the fourth-order) are given in the crystallographic information file, which has been deposited with the Principal Editor of *Mineralogical Magazine* and is available as Supplementary material (see below).

Structures of minerals of the pearceite–polybasite family consist of two kinds of alternating (0001) slabs, which are  $\sim 6$  Å thick (Fig. 7). One slab type (the *A* module) with a general formula

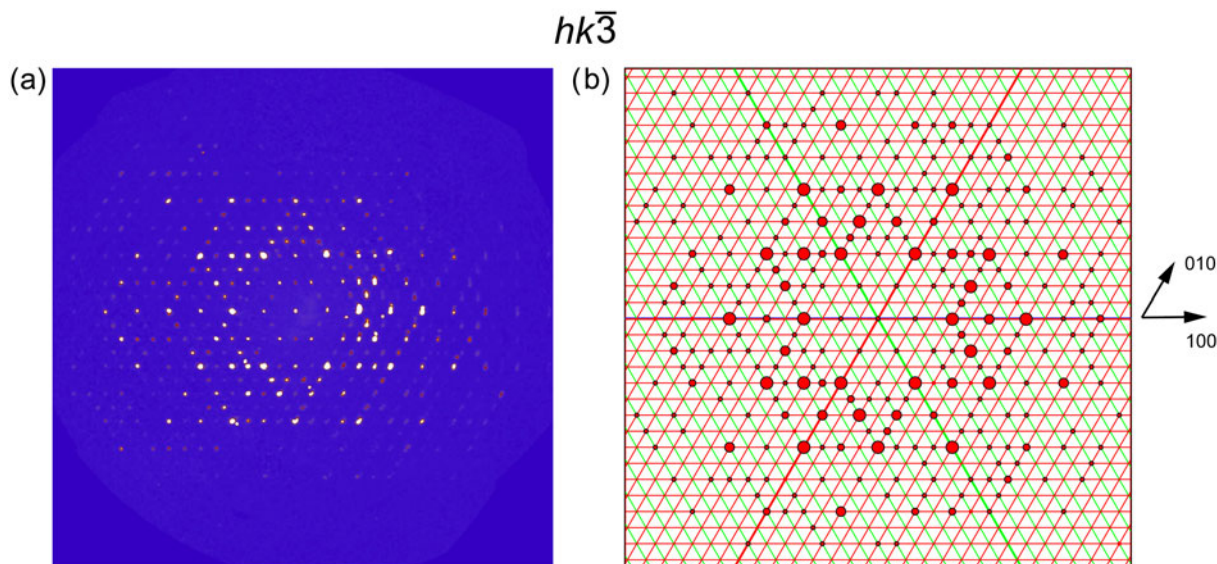


**Figure 6.** Single-crystal diffraction pattern for the argentopolybasite crystal studied. (a) Reciprocal-space reconstruction (by *UNWARP* in *CrysAlisPro*) of the  $hk\bar{3}$  layer, based on experimental diffraction data. (b) Simulated  $hk\bar{3}$  layer of the reciprocal space of argentopolybasite. Reflections from all four domains overlap completely and simulate a hexagonal pattern. The green array corresponds to the second twin domain.

**Table 4.** Summary of data collection conditions and refinement parameters for argentopolybasite from Kremnica.

Crystal data	
Summary chemical formula	$\text{Ag}_{15.478}\text{Cu}_{0.204}(\text{Sb}_{1.648}\text{As}_{0.352})\Sigma_{2.000}\text{S}_{10.937}$
Crystal system	Trigonal
Space group	$P\bar{3}21$
Unit-cell parameters: $a$ , $c$ (Å)	15.0646(5), 12.2552(5)
Unit-cell volume (Å <sup>3</sup> )	2408.61(15)
$Z$	4
Calculated density (g/cm <sup>3</sup> )	6.223 (for the formula from the structure)
Data collection	
Crystal size (mm)	0.058 × 0.024 × 0.023
Diffractometer	Rigaku SuperNova with Atlas S2 CCD
Temperature (K)	297
Radiation, wavelength (Å)	$\text{MoK}\alpha$ , 0.71073 (50 kV, 30 mA)
$\theta$ range for data collection (°)	2.28–29.62
Limiting Miller indices	$-20 \leq h \leq 20$ , $-20 \leq k \leq 20$ , $-16 \leq l \leq 16$
Axis, frame width (°), time per frame (s)	$\omega$ , 1.0, 500
Total reflections collected	61962
Unique reflections	4339
Unique observed reflections, criterion	2804, [ $I > 3\sigma(I)$ ]
Absorption coefficient (mm <sup>-1</sup> ), type	15.67; multi-scan
$T_{\min}/T_{\max}$	0.715/1
Data completeness to $\theta_{\max}$ (%), $R_{\text{int}}$	97.00, 0.153
Refinement	
Structure refinement	Full-matrix least-squares on $F^2$
No. of param., restraints, constraints	304, 0, 12
$R$ , $wR$ (obs)	0.0741, 0.1747
$R$ , $wR$ (all)	0.1029, 0.1873
GOF obs/all	2.17, 1.83
Weighting scheme, weights	$\sigma$ , $w = 1/(\sigma^2(I) + 0.0036I^2)$
Largest diffraction peak and hole (e <sup>-</sup> /Å <sup>3</sup> )	3.49, -1.07
Friedel pairs	1904
Twin fractions 1, 2, 3	0.50(12)/0.227(2)/0.33(12)
Twin matrices /1, 2, 3/	$\begin{pmatrix} 1 & 1 & 0 \\ -1 & 0 & 0 \\ 0 & 0 & 1 \end{pmatrix}, \begin{pmatrix} 1 & 0 & 0 \\ 0 & 1 & 0 \\ 0 & 0 & -1 \end{pmatrix}, \begin{pmatrix} 0 & -1 & 0 \\ -1 & 0 & 0 \\ 0 & 0 & 1 \end{pmatrix}$

$(\text{Ag,Cu})_6(\text{Sb,As})_2\text{S}_7$  has fully occupied pyramidal (As,Sb) positions, with lone electron pairs oriented into the slab and forming a small lone-electron-pair micelle. Ag atoms are located close to the surfaces of this slab, in fully occupied trigonal planar coordinations. Sulfur atoms on the surfaces of the *A* module are coordinated to the silver atoms in both the *A* and *B* module.

The *B* module, with the formula generally given as  $\text{Ag}_9\text{MS}_4$ , where *M* is usually Cu, does not have sites to host the atoms of

**Table 5.** Atom positions, occupancies and equivalent displacement parameters (in Å<sup>2</sup>) for argentopolybasite from Kremnica.

Atom	Wyckoff	$x/a$	$y/b$	$z/c$	$U_{\text{eq}}$
Ag1	6g	0.3668(3)	0.4290(3)	0.1086(3)	0.0456(10)
Ag2	6g	0.0862(2)	0.4230(3)	0.1370(2)	0.0793(14)
Ag3	6g	0.0750(2)	0.1455(3)	0.1220(3)	0.0838(17)
Ag4	6g	0.5692(3)	0.4222(4)	0.1200(4)	0.0697(14)
Ag5	6g	0.3361(5)	0.5444(5)	0.3795(4)	0.129(3)
Ag6	6g	0.4327(15)	0.1273(17)	0.3785(10)	0.075(13)
Ag6'	6g	0.2547(18)	0.0726(10)	0.384(6)	0.216(9)
Ag7	6g	0.1326(8)	0.1775(9)	0.3815(6)	0.196(7)
Ag8	6g	0.633(2)	0.1860(11)	0.3799(6)	0.581(18)
Ag9	6g	0.0756(7)	0.3994(7)	0.3920(5)	0.161(6)
Ag10	6g	0.3833(12)	0.3254(6)	0.3727(7)	0.367(10)
Ag11*	3f	0	0.5109(3)	1/2	0.049(2)
Cu12*	1b	0	0	1/2	0.045(4)
Sb1*	2d	0.333333	0.666667	0.0950(3)	0.0248(10)
Sb2*	6g	0.33403(15)	0.16044(10)	0.09377(13)	0.0280(7)
S1	6g	0.2664(5)	0.5091(5)	0.1893(6)	0.035(3)
S2	6g	-0.0088(4)	0.2379(6)	0.2004(4)	0.034(3)
S3	6g	0.2599(5)	0.2499(5)	0.1784(5)	0.035(3)
S4	6g	0.4915(5)	0.2423(5)	0.1922(6)	0.035(3)
S5	6g	0.5003(4)	0.5001(4)	0.3174(5)	0.031(2)
S6	2c	0	0	0.3179(13)	0.042(4)
S7	6g	0.1843(4)	0.3372(5)	0.4724(4)	0.030(2)
S8	2d	0.333333	0.666667	0.5246(8)	0.029(3)
S9	3e	0.5322(6)	0.5322(6)	0	0.057(4)
S10	3e	0.033 (2)	0.033 (2)	0	0.047(10) **

\*Refined occupancies: Ag6 = 0.181(8), Ag6' = 0.794(8), Ag11 = 0.687(10)Ag, Cu12 = 0.82(3)Cu, Sb1 = 0.73(3)Sb/0.27(3)As, Sb2 = 0.854(19)Sb/0.146(19)As, S10 = 0.25.

\*\*Refined with isotropic atomic displacement parameter.

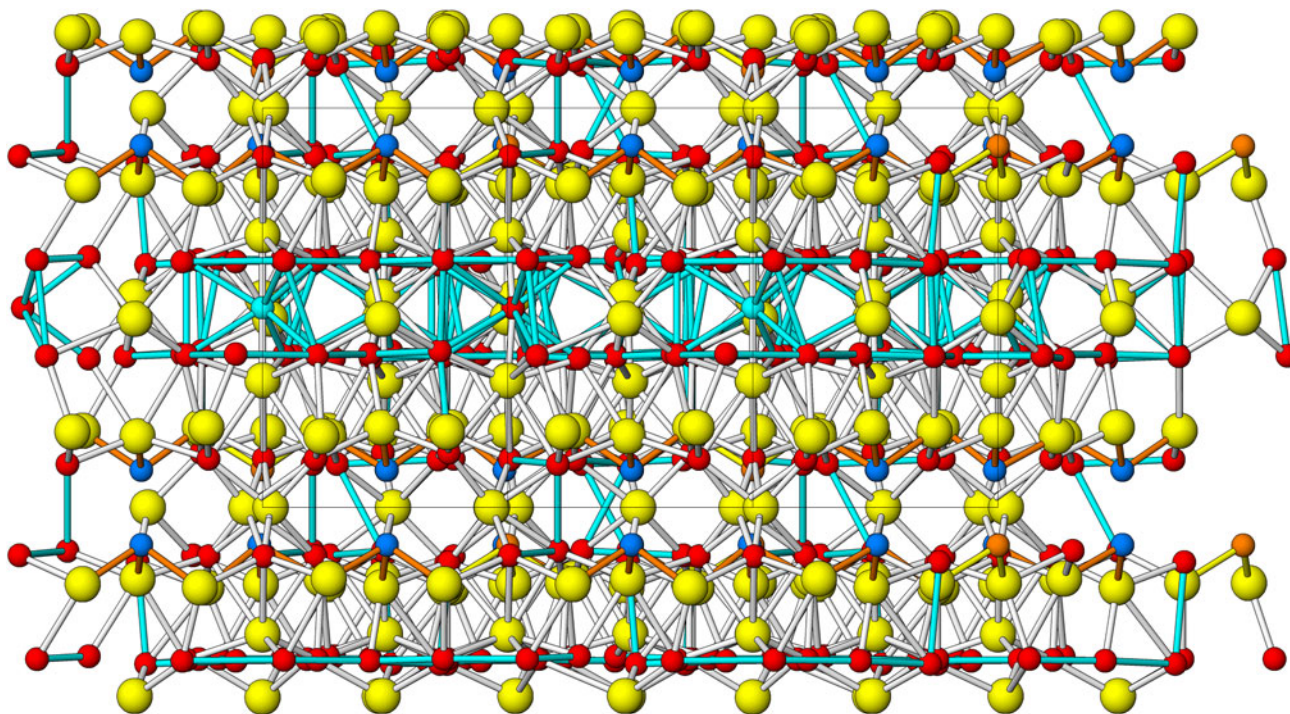


**Figure 7.** Projection of the crystal structure of argentopolybasite on (100). The trigonal  $c$  direction is oriented towards the top of the figure. The (0001) oriented  $A$  module is at  $z$  equal to 0 and 1, the  $B$  module at  $z = \frac{1}{2}$ . Yellow spheres are S atoms, red spheres Ag atoms, the small blue sphere in the  $B$  module is the Ag12 position. In the  $A$  module, blue spheres are Sb (brown bonds) and light brown spheres are As. The median planes of both module types contain less frequent S atoms.

semi-metals. It consists of two mutually interconnected (0001) rings of, in part highly smeared, silver residence sites, which are flat-capped, and separated from the  $A$  modules, by sulfur atoms. One set of silver-occupied rings surrounds a metal site in a special position, which shares the flat sulfur caps applied from both sides. Though in general the (Cu, Ag) site can be differentiated into separate Cu-dominant and Ag-dominant sites (Bindi and Menchetti 2009) the composition of the Nová Baňa sample studied suggests pure Ag occupancy.

Bindi *et al.* (2007c) introduced a simplified nomenclature for the pearceite–polybasite group, with a simple As/Sb rule for the choice of the root name for the (Ag, Cu) phase, and a suffix that indicates the polytype (polytypoid). The latter is one of the three varieties known for this group: *Tac*, *T2ac*, or *M2a2b2c*.

Argentopolybasite complicates this classification by having compositions up to a pure silver mineral, without copper substitution. Notwithstanding, it was found to be rational to maintain the As/Sb criterion and the polytype suffix when naming it. It is a very antimony-rich phase, with known As contents decreasing from 31 to only 11% of the (Sb + As) at.% total, while preserving a well-defined space available for the lone electron pair of Sb.

The number and character of Ag sites is very similar to pearceite-*T2ac*, but the linear-bonded 'B' site is pure silver, with two bonds, which are 2.228 Å long (Fig. 8) in the structurally analysed sample (Table 6), instead of 2.156–2.157 Å, which would be the values typical for linear-bonded Cu. This leads to a more regular  $B$  slab than that observed in the polybasite-series minerals with mixed (Cu,Ag) populations, in which the linear coordinations of Ag and Cu alternate (Bindi and Menchetti 2009). It also yields a longer  $c$  parameter than in other phases of the group. Interestingly, the latter does not hold for the  $a$  parameter, for which the published data indicate that it chiefly depends on the

Sb/As ratio in the mineral (Bindi *et al.*, 2007c). Perhaps, this difference is connected with the adjustability of the (typically) irregular low coordination number Ag–S coordinations in the structure. In agreement with the near-pure Ag-composition, the subcell volume of argentopolybasite exceeds slightly those of other polybasite samples quoted by Bindi *et al.* (2007a, 2007c).

It should be stressed that the average Ag–S distance in the linear-coordinated sites in the  $B$  module is reduced from the typical Ag–S bond length ( $>2.4$  Å) to a value tolerable by the structure. The Ag–S coordinations of the other Ag sites vary between (quasi)linear, triangular, and skewed tetrahedral (3 + 1), with Ag–S bond lengths starting at  $\sim 2.4$  Å and increasing through the increasing coordination (Figs 9, 10, 11). The high values of displacement parameters, especially for Ag8 and Ag10, but also for Ag6, Ag7 and Ag9, indicate high mobility of silver atoms in the structure at ambient conditions.

## Details of the module architecture

### *A* module

The  $A$  module has surfaces densely occupied by sulfur atoms with very similar  $z$  coordinates, and a sparsely occupied median plane, which contains S9 and S10. The (Sb,As) $S_3$  pyramids point inwards and are distributed alternatively on the module surfaces (Fig. 7). Their S atoms overlap in projection on (0001) and create a false impression of a hexagonal net. In its mesh, Ag atoms are concentrated; each bond to two sulfur atoms of the  $SbS_3$  pyramid.

There are two possible descriptions of the coordinations of Ag atoms. On the one hand, they form six-fold cation clusters placed in the false mesh of the Sb coordinations. These are octahedral clusters formed by a combination of Ag1, Ag2 and Ag4 around

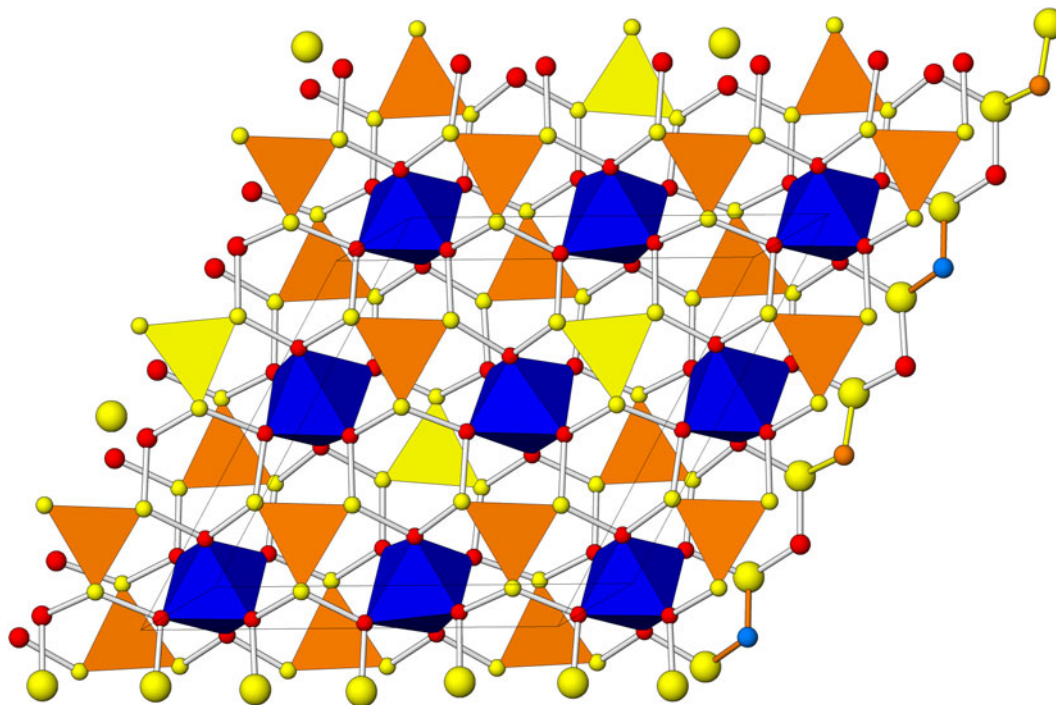


**Figure 8.** Projection of the *A* module on to (0001). The (Sb,As)<sub>3</sub>S<sub>3</sub> pyramids are shown schematically by their S<sub>3</sub> bases, The SAg<sub>6</sub> octahedra are coloured in blue, with S hidden in their centre.

a centrally positioned S9 position (Fig. 8). The Ag–Ag distances are 3.118–3.384 Å. On the other hand, each Ag atom forms triangular AgS<sub>3</sub> co-ordinations which become combined in spinners of six AgS<sub>3</sub> triangles, always by sharing a common S9 atom (Fig. 9). Each spinner consists of two triangular coordinations of Ag1, two of Ag2, and two of Ag4. In the special position  $x = y$ , however, another spinner is formed, centred by a cluster of very closely packed partial S10 positions. It is formed exclusively by Ag3 present in all its triangular coordinations (Fig. 9). The reason for the latter configuration is not clear; it might be a compensation of distinctive dimensions of the two structural modules, *A* and *B*. Mixing of Cu and Ag ligands as the reason

for a disorder of centring sulfur, suggested by Withers *et al.* (2008), does not work for the purely silver-based structure which we refined. It also might be a compromise required by the Sb–As framework because the central region around Ag3 concentrates higher amounts of arsenic, alleviating the degree of overlap. The Ag–S distances in the spinner arms range from 2.407 Å to 2.556 Å, whereas in the S10 cluster they range from 2.460 to 2.725 Å, when we leave out some anomalous extreme values, which result from overlaps (Table 6). The volume of the *A* slab consumed by spinners is illustrated in Fig. 10.

In sulfides, silver commonly occurs with coordinations more complicated than purely triangular. The simplest of them is

**Table 6.** Selected interatomic distances (in Å) in argentopolybasite from Kremnica.

<b>A layer</b>									
Sb1–S1	2.365(7)	Ag1–S1	2.559(10)	Ag2–S1	2.537(7)	Ag3–S2	2.492(10)	Ag4–S4	2.515(9)
Sb1–S1 <sup>ii</sup>	2.365(7)	Ag1–S3	2.502(7)	Ag2–S2	2.537(7)	Ag3–S3	2.516(7)	Ag4–S4 <sup>iv</sup>	2.530(10)
Sb1–S1 <sup>vi</sup>	2.365(11)	Ag1–S5	3.096(7)	Ag2–S5 <sup>vi</sup>	3.069(9)	Ag3–S6	3.062(10)	Ag4–S5	3.086(9)
		Ag1–S9	2.554(7)	Ag2–S9 <sup>vi</sup>	2.416(11)	Ag3–S10	2.11(2)	Ag4–S9	2.479(11)
Sb2–S2 <sup>ix</sup>	2.377(5)					Ag3–S10 <sup>viii</sup>	2.47(2)		
Sb2–S3	2.376(9)	S10–S10 <sup>viii</sup>	0.86(4)			Ag3–S10 <sup>ix</sup>	2.78(2)		
Sb2–S4	2.383(7)	S10–S10 <sup>ix</sup>	0.86(4)						
<b>B layer</b>									
Ag5–S1	2.502(9)	Ag6–S2 <sup>xi</sup>	3.293(14)	Ag6′–S2 <sup>ix</sup>	2.429(11)	Ag7–S2	3.497(15)	Ag8–S4 <sup>xi</sup>	2.817(18)
Ag5–S5	2.965(11)	Ag6–S4	2.739(19)	Ag6′–S6	3.52(3)	Ag7–S3	2.995(10)	Ag8–S5 <sup>xi</sup>	2.613(14)
Ag5–S7	3.022(8)	Ag6–S5 <sup>xi</sup>	2.68(3)	Ag6′–S7 <sup>ix</sup>	3.550(15)	Ag7–S6	2.531(10)	Ag8–S7 <sup>xvi</sup>	3.53(3)
Ag5–S8	2.576(10)	Ag6–S7 <sup>xii</sup>	2.72(2)	Ag6′–S7 <sup>xii</sup>	2.315(11)	Ag7–S7	2.400(14)	Ag8–S8 <sup>xii</sup>	2.330(16)
						Ag7–S7 <sup>xii</sup>	3.521(14)		
Ag9–S1	3.523(10)	Ag10–S3	2.880(12)	Ag11–S5 <sup>vi</sup>	2.244(6)				
Ag9–S2	3.155(10)	Ag10–S4	3.343(15)	Ag11–S5 <sup>xiv</sup>	2.244(6)				
Ag9–S5 <sup>vi</sup>	2.480(15)	Ag10–S5	2.420(9)	Ag11–S7 <sup>vi</sup>	3.991(7)	Cu12–S6	2.230(12)		
Ag9–S7	2.463(14)	Ag10–S7	3.319(17)	Ag11–S7 <sup>xiv</sup>	3.991(11)	Cu12–S6 <sup>xii</sup>	2.230(12)		
		Ag10–S7 <sup>xii</sup>	2.670(10)						

Symmetry codes: (i)  $y, x, -z$ ; (ii)  $-y+1, x-y+1, z$ ; (iii)  $x-y+1, -y+1, -z$ ; (iv)  $-x+y+1, -x+1, z$ ; (v)  $-x, -x+y, -z$ ; (vi)  $-x+y, -x+1, z$ ; (viii)  $-y, x-y, z$ ; (ix)  $-x+y, -x, z$ ; (xii)  $-y+1, x-y, z$ ; (xiii)  $y, x, -z+1$ ; (xiv)  $x-y, -y+1, -z+1$ ; and (xv)  $x-y, -y, -z+1$ .

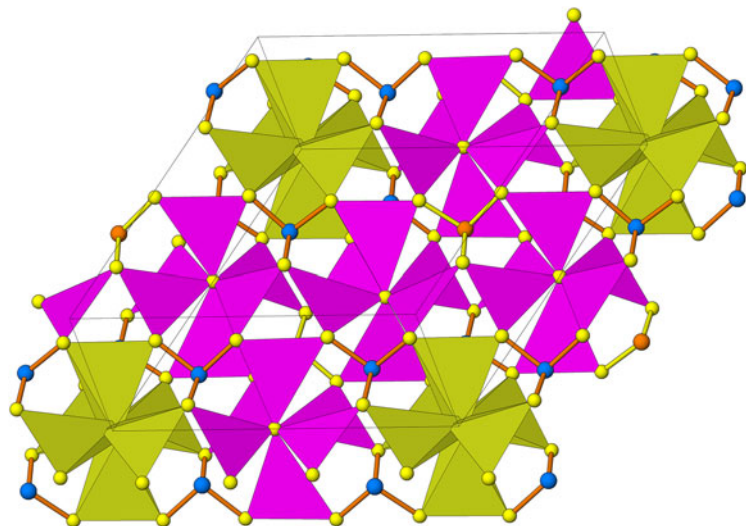


**Figure 9.** The coordination triangles  $\text{AgS}_3$ , which constitute the *A* module, form six-fold spinners centred by S9 (red clusters) and by S10 (hidden, in green clusters). The  $(\text{Sb,As})\text{S}_3$  coordination pyramids are rendered in a ball-and-stick form (Sb blue and As brown). Oblique view.

describable as  $[3 + 1]$ , although the first three distances usually are not equal to one another. However, the additional Ag–S contacts in the *A* module are longer than the known Ag–S bond length. Only Ag2 shows an additional distance below 3.1 Å ( $\text{Ag2-S5} = 3.063$  Å). When this criterion is applied, in each spinner two Ag2 triangles change into two Ag2-based irregular tetrahedra. The Ag3 spinner is not altered by this generalisation.

The spinners present in argentopolybasite (and argento pearceite) are not identical to those in minerals of the tetrahedrite-tennantite series (e.g. Biagioni *et al.*, 2020). In the latter, the opposing ‘wings’ (which are oriented at  $180^\circ$  to one another) are perpendicular to one another, whereas in the former their planes are parallel.

### *B* module

The *B* module has the median plane populated sparsely by the following sulfur atoms (Fig. 7): S6 situated at the 0,0 site, S5 on the cell edges and in the cell centre, furthermore S8 which is positioned on the threefold rotation axes, and the six S7 positions, which surround the 0,0 point in the median plane. For S6,

there is a short Ag–S distance to Ag12 (2.228 Å long), and six Ag7–S distances (2.564 Å long). The S5 atom has a pair of 2.246 Å distances to Ag11, 2.630 Å to Ag8, and 2.479 Å to Ag9. It also has S7 fourfold-coordinated, at 2.329–2.716 Å. The Ag–Ag bonding scheme of the *B* module was investigated by examining the presence of distances below 2.8 Å. Only the Ag6–Ag8 (2.710 Å), Ag6–Ag9 (2.670 Å), Ag6–Ag6′ (2.390 Å) and Ag10–Ag11 (2.689 Å) distances satisfy this criterion.

The *B* module can be described as composed of four kinds of coordination polyhedra, with Ag as the only ligand in all of them. Two of these polyhedra are cation-centred, by Ag12 and Ag11, respectively, whereas a further two are anion-centred, by S8 and S7, respectively (Figs 11, 12).

The trigonal antiprism centred by Ag12 (Fig. 13) has six Ag7 atoms as ligands, with cation–cation contacts of 2.836 Å to Ag12, and 2.987 Å increasing to >4.300 Å for Ag7–Ag7. The occupancy of the central cation (refined as 0.820 Cu) has to be taken as 0.51 Ag, an extremely vacant cation position. Through the two horizontal faces of the  $[\text{Ag12}](\text{Ag7})_6$  coordination octahedron, two short Ag12–S6 bonds of only 2.228 Å form, resulting in a linear sulfur–cation–sulfur bonding scheme. With the *z* coordinate

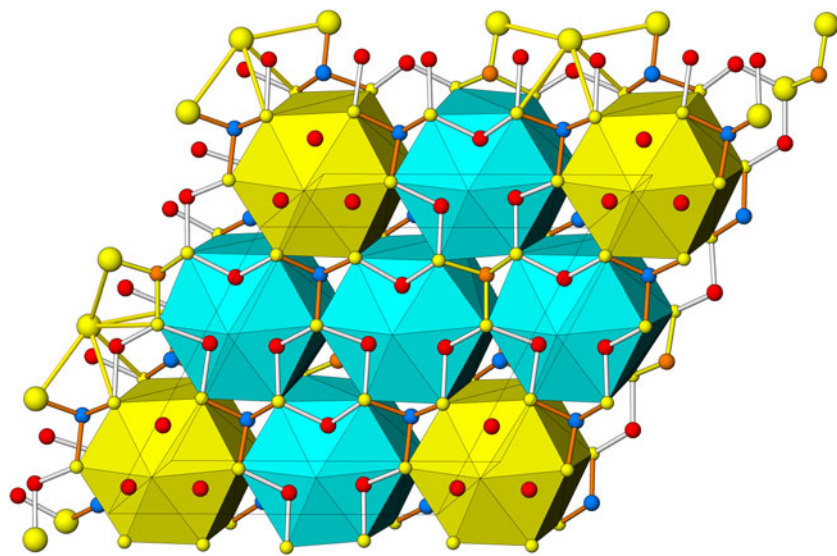


**Figure 10.** Volumes in the *A* module, which are occupied by the spinners of Ag–S triangles (shown in Fig. 9). They are centred by S9 (blue polyhedra) and by S10 (yellow polyhedra).



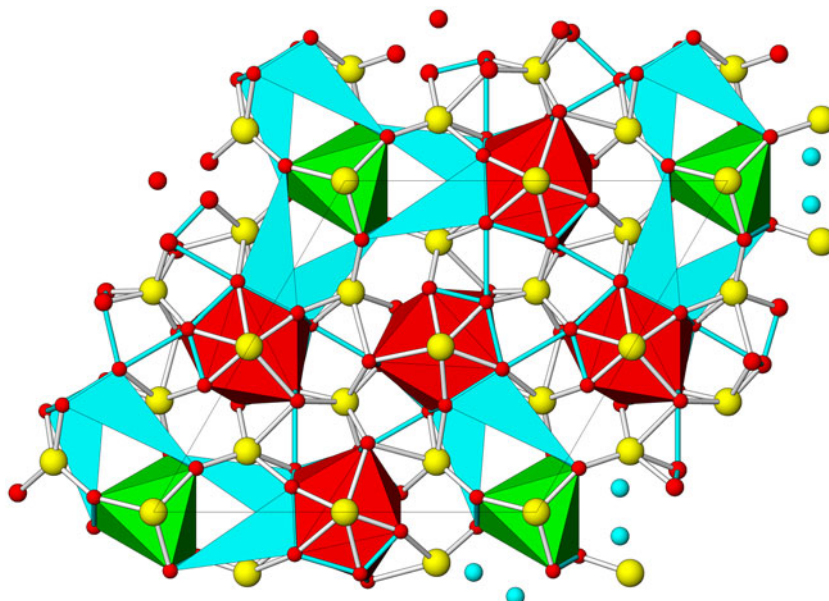


**Figure 11.** The silver-centred coordination polyhedra in the B layer of argentopolybasite with silver ligands: 10-fold, 6-fold and 3-fold coordination (Ag–S distances up to 3.3 Å included). Colouring: brown, green and light blue (this one only short bonds), respectively; all polyhedra are capped by S atoms.

comparable to that of Ag12, there are four S7 atoms at 4.416 Å. These are the only anions in the vicinity of Ag12. The two ‘topping’ S6 atoms, which ‘top’ the [Ag12](Ag7)<sub>6</sub> polyhedron along [0001], have umbrella-like bonds to Ag7 (2.564 Å). The Ag–Ag distances that cross the S7-filled median plane of the module obliquely are ~2.987 Å. On the outside of the Ag12-based group, there is a horizontal distance for Ag6–Ag9 of 2.670 Å, present on both *z* levels, which are occupied by the silver atoms.

The trigonal antiprism centred by Ag12 (Fig. 13) has six Ag7 atoms as ligands, with cation–cation contacts of 2.836 Å to Ag12, and 2.987 Å increasing to >4.300 Å for Ag7–Ag7. The occupancy of the central cation (refined as 0.820 Cu) has to be taken as 0.51 Ag, an extremely vacant cation position. Through the two horizontal faces of the [Ag12](Ag7)<sub>6</sub> coordination octahedron, two short Ag12–S6 bonds of only 2.228 Å form, resulting in a linear sulfur–cation–sulfur bonding scheme. With the *z* coordinate

comparable to that of Ag12, there are four S7 atoms at 4.416 Å. These are the only anions in the vicinity of Ag12. The two ‘topping’ S6 atoms, which ‘top’ the [Ag12](Ag7)<sub>6</sub> polyhedron along [0001], have umbrella-like bonds to Ag7 (2.564 Å). The Ag–Ag distances that cross the S7-filled median plane of the module obliquely are ~2.987 Å. On the outside of the Ag12-based group, there is a horizontal distance for Ag6–Ag9 of 2.670 Å, present on both *z* levels, which are occupied by the silver atoms.

The Ag11-centred coordination polyhedron (Fig. 14) is an irregular antiprism that consists of the central Ag11 atom (at *z* = 0.5, *x* = 0 and *y* ≈ 0.5) and of two *z* levels, both occupied by Ag10, Ag9, Ag8 and Ag5. This coordination polyhedron exhibits a twofold rotation symmetry. The Ag–Ag distance is 2.800 Å for Ag9–Ag11, 2.689 Å for Ag10–Ag 11, 2.868 Å for Ag8–Ag11 and 3.159 Å for Ag5–Ag11; each of them occurs twice in this polyhedron (Fig. 15). Across the difference in the *z* coordinate, the

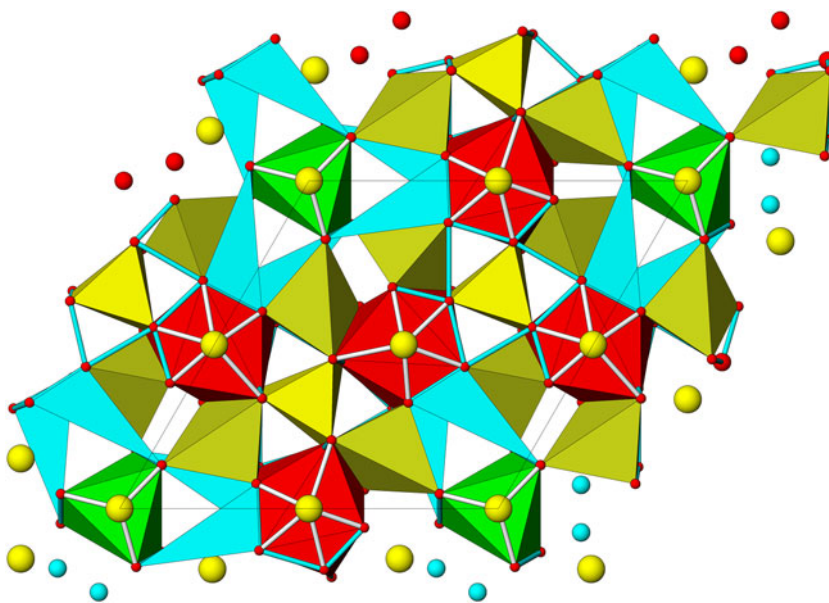


**Figure 12.** Combination of the Ag-centred and S-centred coordination polyhedra (all with Ag as ligands) in the B layer. The S-centred polyhedra, which were added to the contents of Fig. 11 are indicated in yellow and khaki-yellow tones.

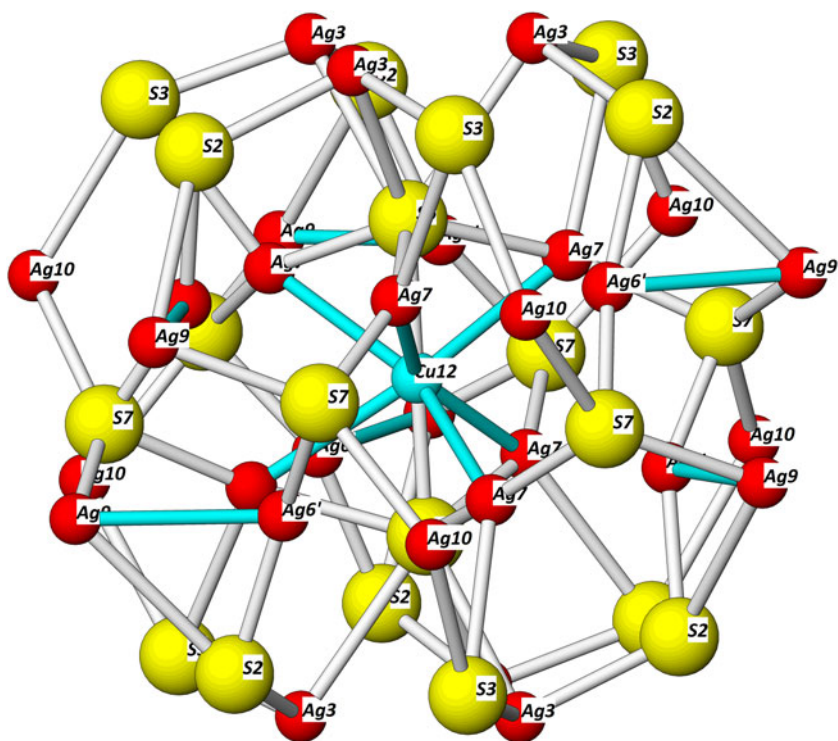


**Figure 13.** Environment of the (Ag,Cu)12-centred cluster of silver atoms in argentopolybasite. S in yellow, Ag in red. Short Ag–Ag interactions are indicated by blue joins.

Ag10–Ag10 distance is 3.469 Å and the Ag8–Ag9 distance is 2.987 Å.

The question of unusually short bonds in the two linear (Ag,Cu)–S bonding schemes has been presented as a result of Cu presence and Cu–Ag mixing in the central site of the metal polyhedron, e.g. by Bindi *et al.* (2006, 2015a) for pearceite and

for cupropearceite from Tsumeb, respectively. The latter compound has 1.0 Cu in the site and the linear coordination of 2.151 Å Cu–S bonds. However, our studies of the almost pure Ag members of the group show that in the argentopolybasite studied the Ag11 site has occupancy of only 0.674 atoms and the Ag12 site has been refined as 0.51 Ag. This site perhaps

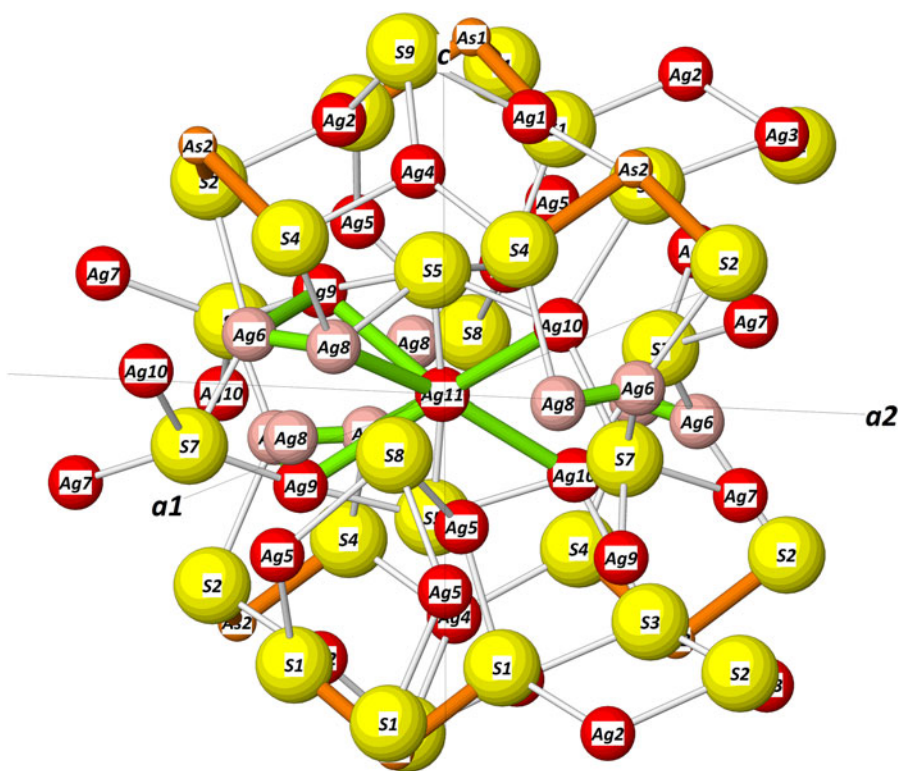


**Figure 14.** Environment of the Ag11-centred cluster of silver atoms in argentopolybasite. S in yellow, Ag in red. Short Ag – Ag interactions are indicated by green joins.

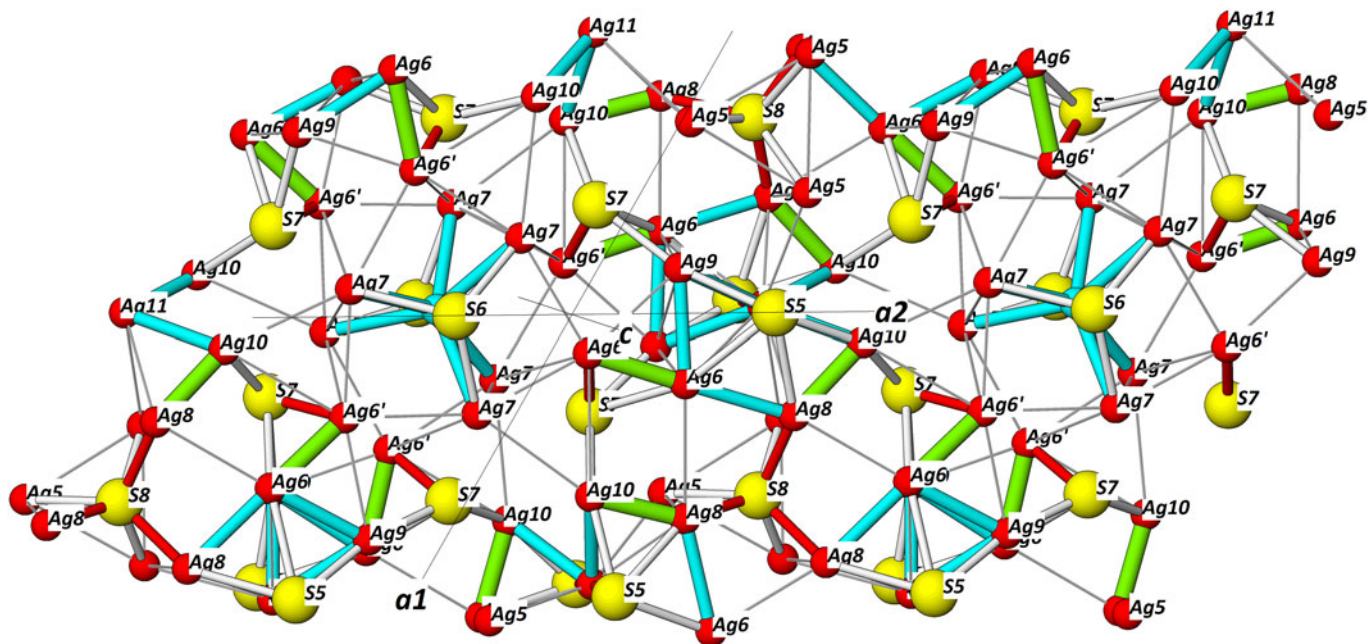


**Figure 15.** Distribution of silver–silver interactions in the *B* module of argentopolybasite: strong interactions (Ag–Ag distances 2.51–2.86 Å) are rendered in light blue, anomalously short interactions (distances below 2.51 Å) in green, and weak interactions (2.86–3.40 Å) as thin grey interconnections. Ag–S bonds of usual Ag–S length are indicated as white sticks, the anomalously short ones as red interconnections.

also collects traces of copper in mixed-metal cases. In pure Ag-argentopearceite (Sejkora *et al.*, unpublished data), these site occupancies were 0.78 and 0.74, in the same order. This suggests the possibility of partial vacancies in these sites of the pearceite-polybasite group, even if crystal structures of some of these minerals were refined with fully occupied mixed linear-coordinated Ag–Cu sites. This situation also influences the calculated local charge distributions.

In projection on (0001), the coordination assembled around Ag11 resembles a pentagonal prism, with one distant vertex and one skewed edge (Figs 11, 15). The most vexing problem is to explain the ‘escape’ of the bulk of ‘Ag6 silver’ from the Ag6 position in the

half-circle (occupancy 0.181 Ag per site) to the extended site Ag6' (occupancy 0.794 Ag). Anisotropic displacement ellipsoids suggest the avoidance of close contacts between these two positions rather than overflow from one position to another. Each new position forms a short bond with S7 in an elongated structure space, which itself is lined up by Ag7, Ag10 and an Ag9–Ag6 rectangle – this ‘escape’ might be a trend to occupy a site with a more advantageous charge compensation than the original Ag6 position.

The S8-centred distorted octahedron (Fig. 12) has Ag5–S8 bonds 2.583 Å long and three more distances Ag8–S8, which are 2.334 Å long. Its central anion is the only anion in a circle formed by three S5 pairs and the intervening S7 and S8 atoms;

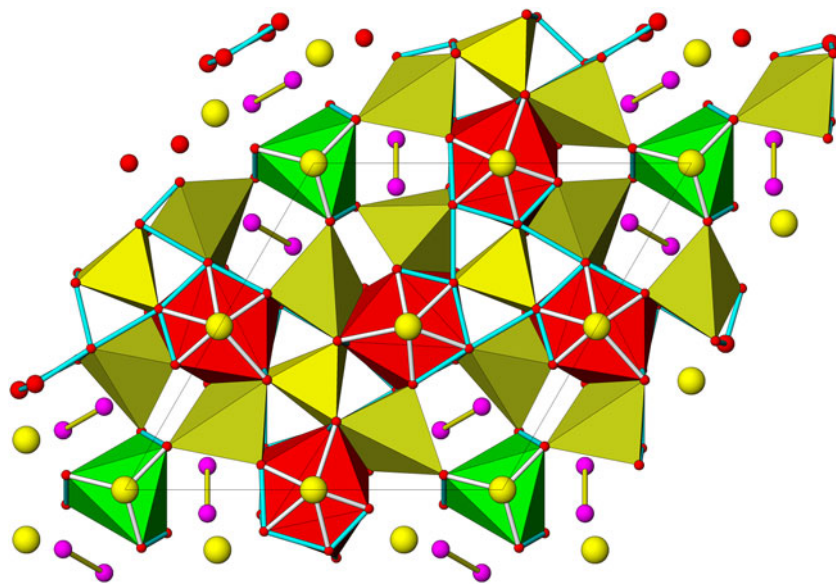


**Figure 16.** Polyhedral scheme of the *B* module (see Figs 11, 12) with the silver Ag6' positions (small red spheres). Their elevation difference (3.416 Å) is indicated by a connecting stick across the vacated S7-centred polyhedron.

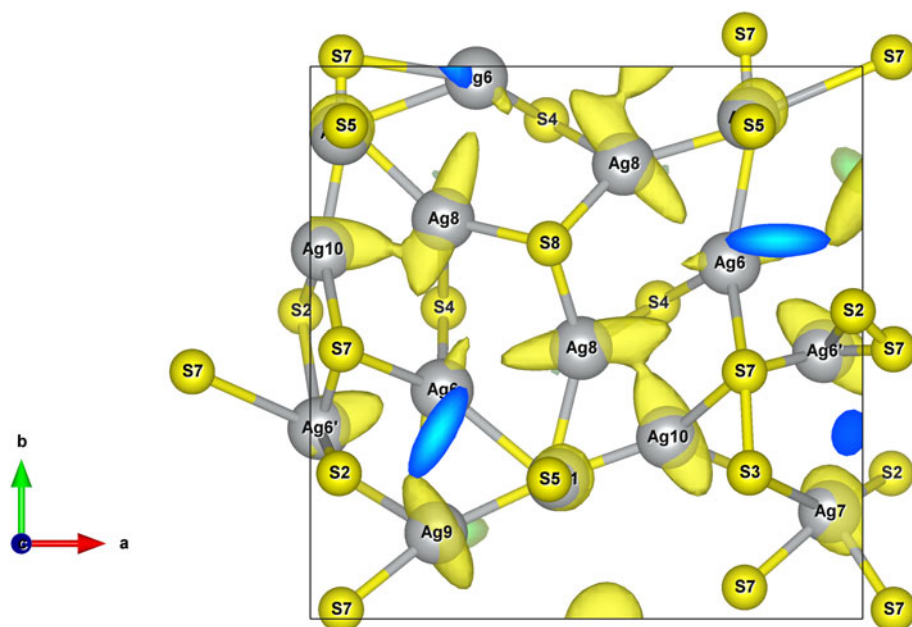


**Figure 17.** An individual (0001) slab of silver atoms of the *B* module at the ambient temperature, at which X-ray diffraction took place, with the anisotropic displacement parameters applied. Selection of the *z* level which contains Ag6–Ag8–Ag9–Ag10 and further details of the configuration as well as the explanations of the observed phenomena are in the text.

this has influence on the cation charge distribution in the module. The S7-centred quasi-pyramid, built by Ag ligands, is much less regular, with six faces of a different character. The shortest bonds in this polyhedron vary as 2.329, 2.372 and 2.465 Å, with additional 2.680 and 2.70 Å (Table 6). The polyhedra centred by S8 and S7 join together, forming triangular aggregates, with the S8-centred polyhedron in the group centre. These groups are interspaced by cation-centred polyhedra (Fig. 12). Fig. 16 shows that the ‘escape’ site Ag6’ (see above) is a part of the S7-based polyhedron, with the spacing between the symmetry-related Ag6’ sites beyond the range of cation–cation interactions, at 3.416 Å.

Similar interspacing of cation-centred and sulfur-centred polyhedra takes place in the direction perpendicular to the (0001) layers. In the [0001] column passing through the origin of the unit cell, the Ag12-centred octahedra formed by Ag7 ligands, with two additional S6 atoms protruding along the  $\pm[0001]$  direction, alternate with the S-centred (S10)(Ag3)<sub>6</sub> octahedra sandwiched between rings of As2 pyramids. In the [0001] column positioned on a combined S5-and-S9 string, the Ag11-centred cation clusters of six assorted Ag atoms alternate with S9-centred octahedra, the ligands of which belong to the Ag1, 2 and 4 silver sites. The latter is surrounded by a ring formed by two As2 and one As1 pyramid; Ag5 is at a longer distance from Ag11.

### The mobile component

At the ambient temperature, at which X-ray diffraction took place, the most interesting anisotropic displacement phenomena take place in the individual (0001) layers of silver atoms of the *B* module (Fig. 17). They involve Ag6, Ag8, Ag9 and Ag10, which form, in this plane, a four-member half-circular group. Among them, only the Ag8–Ag10 pair demonstrates an unusually short Ag–Ag distance (2.240 Å), as also does the Ag6–Ag6’ pair (spacing 2.390 Å). The latter has the Ag6’ position attached externally to the half-circular group (Fig. 15). The Ag8 and Ag6 atoms around the S8 site show no confluence, nor do Ag6’ and Ag6

(Fig. 17). The atom displacement ellipsoid of Ag6’ is subparallel to those of Ag9 and Ag10.

The displacement ellipsoids of the quoted atoms do not form a polygon which would suggest a mobile arrangement for Ag along the Ag6, Ag8, Ag9 and Ag10 paths. Instead, the large ellipsoid of Ag10 points towards the geometric focus of the ellipsoid of Ag8, and that of Ag8 points to the focus of the ‘undernourished’ displacement ellipsoid of Ag6 (Fig. 17). This suggests another mobility mechanism: the static Ag–Ag (ellipsoid centre–ellipsoid centre) distances of these two pairs of silver atoms are too short but when in a given moment the Ag8 atom is at the ellipsoid corner distant from the Ag10 ellipsoid, the equilibrium distance to Ag10 is preserved, even when Ag10 at the same moment approaches the ellipsoid of Ag8. The same is true for the opposite case, with Ag8 close to the tip of the Ag10 ellipsoid, and Ag10 being at the distant end of its own displacement ellipsoid: it means that the vibrations of these two atoms are synchronised. This might be true also for the Ag6–Ag6’ pair and the Ag6’–Ag9 pair in some orientations, etc. (Fig. 17). Quite possibly, the vibrations of Ag atoms in the entire (001) plane are synchronised, at least as larger domains.

The Ag11 silver atom shows no signs of disorder. Transverse displacements of Ag8 and Ag6’ result in reduced Ag8–S8 and Ag6’–S7 distances which were mentioned above.

The difference compared to argentopearceite is conspicuous – the As-rich analogue nearly lacks the mobility of Ag, perhaps because of spatial (potential path/volume) problems. In argentopearceite, Ag8, Ag11 and Ag12 show only ellipsoidal atom displacements in the (0001) plane, whereas Ag9 in argentopearceite is oriented out of this plane – it appears to have vibrations coordinated with those of its linear-coordinated Ag10 (Sejkora *et al.*, unpublished data).

### Relationship to the known species

Argentopolybasite is a member of the polybasite group, Strunz class 2.GB.15. According to the valid nomenclature for this group (Bindi *et al.*, 2007c) its members exhibit the general

**Table 7.** Comparison of argentopolybasite and other Sb–S–dominant members of the polybasite group.\*

Mineral	argentopolybasite	polybasite	polybasite	polybasite	cupropolybasite
Polytype	<i>T2ac</i>	<i>T2ac</i>	<i>M2a2b2c</i>	<i>Tac</i>	<i>Tac</i>
ML-A <i>M</i>	Ag	(Ag,Cu)	Ag	(Ag,Cu)	(Cu,Ag)
ML-A <i>T</i>	(Sb,As)	Sb	Sb	(Sb,As)	(Sb,As)
ML-B “Ag”	Ag	Ag	Ag	Ag	Ag
ML-B “Cu”	Ag	Cu	Cu	Cu	Cu
Cu (wt.%)	0.49	4.76	3.63	8.46	14.63
Cu (apfu)	0.18	1.69	1.29	2.91	4.82
Space group	<i>P321</i>	<i>P321</i>	<i>C2/c</i>	<i>P3m1</i>	<i>P3m1</i>
<i>a</i> (Å)	15.0646(5)	15.094(12)	26.188(3)	7.4805(5)	7.3277(3)
<i>b</i> (Å)			15.1199(18)		
<i>c</i> (Å)	12.2552(5)	11.8825(8)	23.784(3)	11.8836(13)	11.7752(6)
$\beta$ (°)			90.0		
<i>V</i> (Å <sup>3</sup> )	2408.61(15)	2344.9(3)	9418(2)	575.89(8)	547.56(8)
<i>Z</i>					
‘ <i>a</i> ’ (Å)	7.532	7.548	7.560	7.481	7.328
‘ <i>c</i> ’ (Å)	12.255	11.883	11.892	11.884	11.775
‘ <i>V</i> ’ (Å <sup>3</sup> )	602.09	586.30	588.61	575.89	547.56
	this paper	Evain et al. (2006)	Evain et al. (2006)	Bindi et al. (2007a)	Bindi et al. (2007d)

\*Notes: ML-A = module layer A; ML-B = module layer B; ‘*a*’, ‘*c*’ and ‘*V*’ = parameters of hexagonal subcell.

formula  $[M_6T_2S_7][Ag_9CuS_4]$  with *M* = Ag and Cu and *T* = As and Sb and their crystal structure can be described by two pseudolayer modules: module layer *A*  $[M_6T_2S_7]^{2-}$  and *B* one  $[Ag_9CuS_4]^{2+}$ . Members with Sb > As are polybasite, those with As > Sb are pearceite. Subsequently, members with Cu-dominant occupation at *M* position of *A* module layer (i.e. with total Cu contents > 4.00 apfu) have been defined as the minerals cupropolybasite and cupropearceite (Bindi et al., 2007d) and the Se-rich member with formula  $[(Ag,Cu)_6(Sb,As)_2(S,Se)_7][Ag_9Cu(S,Se)_2Se_2]$  as selenopolybasite (Bindi et al., 2007b). More recently, benleonardite  $[Ag_6(Sb,As)_2S_6Te] [Ag_9Cu(S,Te)_2Te_2]$  was recognised as a member of this group (Bindi et al., 2015a).

For the approved members of this group, contents of ~1 apfu Cu at *B* module layer  $[Ag_9CuS_4]$  are usual (Bindi et al., 2006, 2007a, 2007b, 2007c, 2007d; Evain et al., 2006); with only three exceptions. The first is for polybasite-*M2a2b2c* described by Bindi and Menchetti (2009) with only 0.43 apfu Cu (determined by electron probe microanalysis) and 0.50 apfu according to single-crystal data. The second is the case of benleonardite, for which on the basis of single-crystal data alone Bindi et al. (2015a) defined the formula  $[Ag_6(Sb,As)_2S_6Te] [Ag_9Cu(S,Te)_2Te_2]$  though multiple published chemical data show either the total absence [samples from Bambolla and Ivigtut – see Bindi et al., 2015a] or only minimal Cu contents [samples from Bambolla, Emperor, Um Samiuki occurrences – up to 0.31 wt.% (Bindi et al., 2015a) and from Vorontsovskoe deposit up to 0.68 wt.% (Kasatkin et al., 2022)] with Cu < 0.50 apfu. The third case is the first approved Ag-dominant member (Cu in module layer *B* fully substituted by Ag) of the polybasite group, the new mineral argentoppearceite-*T2ac* (IMA2020-049; Sejkora et al., 2020).

The number of individual sites usually occupied by Cu in module layer *B*  $[Ag_9CuS_4]$  in polybasite-group minerals is related to the polytype: one site for *-T2ac*; two for polytype *-T2ac*; and three sites for *-M2a2b2c*. Therefore, we suggest that nomenclature should define simple polybasite as a mineral with Cu > 0.5 apfu and argentopolybasite with Cu < 0.5 apfu. The same limit was approved in the case of pearceite/argentoppearceite (IMA2020-049; Sejkora et al., 2020).

Argentopolybasite is a member of the polybasite group with Cu in module layer *B* substituted by Ag. A comparison of selected data for Sb–S members of the polybasite group is given in Table 7.

## Conclusions

Based on the investigations in three different mineral occurrences, the present study has proved that the polybasite structure and composition could exist without copper substituting specific cation sites of the structure. The formation of Ag-rich clusters separated by S-centred polyhedra is an interesting phenomenon, although the Ag–Ag distances mostly remain just above the known Ag–Ag bond value. In addition, this study revealed interesting atom-to-atom relationships and displacement patterns which indicate synchronisation of atom vibrations in the silver-rich *B* layer of argentopolybasite below the temperatures at which silver becomes fully mobile.

**Acknowledgements.** The helpful comments of Associated Editor Ian Graham and Structural Editor Peter Leverett, as well as two other anonymous reviewers are greatly appreciated. We are also grateful to Radek Škoda for the WDS analysis of the sample from Arykevaam. Pavel Škácha and Maria Milshina are acknowledged for photography. The study was supported financially by VEGA projects 2/0029/23 and 2/0028/20 as well as by the Ministry of Culture of the Czech Republic (long-term project DKRVO 2019-2023/1.II.e; National Museum, 00023272). JP acknowledges the support through the project No. LO1603 under the Ministry of Education, Youth and Sports National sustainability program I of the Czech Republic.

**Competing interests.** The authors declare none.

**Supplementary material.** To view supplementary material for this article, please visit <https://doi.org/10.1180/mgm.2022.141>

## References

- Biagioni C., George L.G., Cook N.J., Makovicky E., Moëlo Y., Pasero M., Sejkora J., Stanley C.J., Welch M.D. and Bosi F. (2020) The tetrahedrite group: Nomenclature and classification. *American Mineralogist*, **105**, 109–122.
- Bindi L. and Menchetti S. (2009) Adding further complexity to the polybasite structure: The role of Ag in the *B* layer of the *-M2a2b2c* polytype. *American Mineralogist*, **94**, 151–155.
- Bindi L., Evain M. and Menchetti S. (2006) Temperature dependence of the silver distribution in the crystal structure of natural pearceite,  $(Ag,Cu)_{16}(As,Sb)_2S_{11}$ . *Acta Crystallographica*, **B62**, 212–219.
- Bindi L., Evain M. and Menchetti S. (2007a) Complex twinning, polytypism and disorder phenomena in the crystal structures of antimonpearceite and arsenopolybasite. *The Canadian Mineralogist*, **45**, 321–333.

- Bindi L., Evain M. and Menchetti S. (2007b) Selenopolybasite,  $(\text{Ag,Cu})_6(\text{Sb,As})_2(\text{S,Se})_7[\text{Ag}_9\text{Cu}(\text{S,Se})_2\text{Se}_2]$ , a new member of the pearceite-polybasite group from the De Lamar mine, Owyhee County, Idaho, USA. *The Canadian Mineralogist*, **45**, 1525–1528.
- Bindi L., Evain M., Spry P.G. and Menchetti S. (2007c) The pearceite-polybasite group of minerals: Crystal chemistry and new nomenclature rules. *American Mineralogist*, **92**, 918–925.
- Bindi L., Evain M., Spry P.G., Tait K.T. and Menchetti S. (2007d) Structural role of copper in the minerals of the pearceite-polybasite group: The case of the new minerals cupropearceite and cupropolybasite. *Mineralogical Magazine*, **71**, 641–650.
- Bindi L., Voudouris, P. and Spry, P.G. (2013) Structural role of tellurium in the minerals of the pearceite-polybasite group. *Mineralogical Magazine*, **77**, 419–428.
- Bindi L., Stanley C.J. and Spry P.G. (2015a) New structural data reveal benleopardite to be a member of the pearceite-polybasite group. *Mineralogical Magazine*, **79**, 1213–1221.
- Bindi L., Topa D. and Frank F.N. (2015b) How much copper can the pearceite structure sustain? The case of cupropearceite from Tsumeb, Namibia. *Periodico di Mineralogia*, **84**, 341–350.
- Böhmer M. (1966) Geology and mineral associations of gold-bearing veins in the central part of the Kremnica ore field. *Acta Geologica et Geographica Universitatis Comenianae, Geologica*, **11**, 5–123 [in Slovak].
- Burnham C.W. (1962) Lattice constant refinement. *Carnegie Institute Washington Yearbook*, **61**, 132–135.
- Chernyshev I.V., Konečný V., Lexa J., Kovalenker V.A., Jeleň S., Lebedev V.A. and Goltzman Y.V. (2013) K-Ar and Rb-Sr geochronology and evolution of the Štiavnica Stratovolcano (Central Slovakia). *Geologica Carpathica*, **64**, 327–360.
- Criddle A.J. and Stanley C.J. (1993) *Quantitative Data File for Ore Minerals*. Third edition. Chapman & Hall, London.
- Evain M., Bindi L. and Menchetti S. (2006) Structural complexity in minerals: twinning, polytypism and disorder in the crystal structure of polybasite,  $(\text{Ag,Cu})_{16}(\text{Sb,As})_2\text{S}_{11}$ . *Acta Crystallographica*, **B62**, 447–456.
- Kasatkin A.V., Stepanov S. Yu., Tsyganko M.V., Škoda R., Nestola F., Plášil J., Makovický E., Agakhanov A.A. and Palamarchuk R.S. (2022) Mineralogy of the Vorontsovskoe gold deposit. *Mineralogy*, **8**, 5–93.
- Kodéra P., Šucha V., Lexa J. and Fallick A.E. (2007) The Kremnica Au-Ag epithermal deposit: an example of laterally outflowing hydrothermal system? Pp. 173–176 in: *Digging Deeper* (Andrew C.J. et al., editors). Proceedings of the IX SGA Conference, Irish Association for Economic Geology, Dublin, Ireland.
- Konečný V., Lexa J., Halouzka R., Hók J., Vozár J., Dublan L., Nagy A., Šimon L., Havrila M., Ivanička J., Hojstričová V., Mihaliková A., Vozárová A., Konečný P., Kováčiková M., Filo M., Marcin D., Klukanová A., Liščák P. and Žáková E. (1998) *Explanations to the Geological Map of the Štiavnické Vrchy and Pohronský Inovec Mountains (Štiavnica Stratovolcano) 1:50 000, I. and II. Part*. Geological Survey of Slovak Republic, Bratislava 473 pp. [in Slovak with English summary].
- Kraus I., Chernishev I.V., Šucha V., Kovalenker V.A., Lebedev V.A. and Šamajová E. (1999) Use of illite for K/Ar dating of hydrothermal precious and base metal mineralization in Central Slovak Neogene volcanic rocks. *Geologica Carpathica*, **50**, 353–364.
- Lexa J. and Bartalšík B. (1999) Low-sulfidation epithermal gold at Kremnica. Pp. 265–273 in: *Epithermal Mineralization of the Western Carpathians* (Molnár, F., Lexa J. and Hedenquist J.W., editors). Society of Economic Geologists, Guidebook Series, **31**.
- Lexa J., Halouzka R., Havrila M., Hanzel L., Kubeš P., Liščák P. and Hojstričová V. (1998) *Explanatory Notes to the Geological Map of the Kremnické Vrchy Mountain Range*. D. Štúr Institute of Geology, Bratislava, 1–308.
- Lexa J., Žáková E., Hojstričová V. and Rojkovičová L. (2002) *The Nová Baňa deposit*. Partial report. Archive State Geological Institute Dionyz Štúr, Bratislava [in Slovak].
- Majzlán J., Berkh K., Kiefer S., Kodéra P., Fallick A.E., Chovan M., Bakoš F., Beroň A., Ferenc Š. and Lexa J. (2018) Mineralogy, alteration patterns, geochemistry, and fluid properties of the Ag-Au epithermal deposit Nová Baňa, Slovakia. *Mineralogy and Petrology*, **112**, 1–23.
- Ondruš P. (1993) A computer program for analysis of X-ray powder diffraction patterns. *Materials Science Forum, EPDIC-2, Enchede*, **133–136**, 297–300.
- Petříček V., Dušek M. and Plášil J. (2016) Crystallographic computing system Jana2006: Solution and refinement of twinned structures. *Zeitschrift für Kristallographie*, **231**, 583–599.
- Petříček V., Dušek M. and Palatinus L. (2020) *Crystallographic computing system Jana2020*. Institute of Physics, CAS, Prague, Czech Republic.
- Pouchou J.L. and Pichoir F. (1985) “PAP” ( $\varphi\rho Z$ ) procedure for improved quantitative microanalysis. Pp. 104–106 in: *Microbeam Analysis* (J.T. Armstrong, editor). San Francisco Press, San Francisco.
- Rigaku (2019) *CrysAlis CCD and CrysAlis RED*. Rigaku-Oxford Diffraction Ltd, Yarnton, Oxfordshire, UK.
- Sejkora J., Plášil J., Makovický E., Škácha P., Dolníček Z. and Gramblička R. (2020) Argentoppearceite, IMA 2020-049. CNMNC Newsletter No. 57. *Mineralogical Magazine*, **84**, <https://doi.org/10.1180/mgm.2020.73>.
- Sheldrick G.M. (2015) SHELXT – integrated space-group and crystal-structure determination. *Acta Crystallographica*, **A71**, 3–8.
- Števkó M., Mikuš T., Sejkora J., Plášil J., Makovický E., Vlasáč J. and Kasatkin A. (2022) Argentopolybasite-T2ac, IMA 2021-119. CNMNC Newsletter 67. *Mineralogical Magazine*, **86**, <https://doi.org/10.1180/mgm.2022.56>.
- Volkov A.V., Prokofiev V. Yu., Sidorov A.A., Galaymov A.L., Wolfson A.A. and Sidorova N.V. (2020) Conditions for the Au–Ag Epithermal Mineralization in the Arykevaam Volcanic Field, Central Chukotka. *Journal of Volcanology and Seismology*, **14**, 220–228.
- Withers R.L., Norén L., Welberry T.R., Bindi L., Evain M. and Menchetti S. (2008) A composite modulated structure mechanism for  $\text{Ag}^+$  fast ion conduction in pearceite and polybasite mineral solid electrolytes. *Solid State Ionics*, **179**, 2080–2089.